



Study of beauty hadron decays into pairs of charm hadrons

R. Aaij, Y. Amhis, S. Barsuk, O. Callot, J. He, O. Kochetina, J. Lefrançois, F. Machefer, A. Martin Sanchez, M. Nicol, et al.

► To cite this version:

R. Aaij, Y. Amhis, S. Barsuk, O. Callot, J. He, et al.. Study of beauty hadron decays into pairs of charm hadrons. *Physical Review Letters*, 2014, 112, pp.202001. 10.1103/PhysRevLett.112.202001 . in2p3-00959851

HAL Id: in2p3-00959851

<https://hal.in2p3.fr/in2p3-00959851>

Submitted on 12 Sep 2023

HAL is a multi-disciplinary open access archive for the deposit and dissemination of scientific research documents, whether they are published or not. The documents may come from teaching and research institutions in France or abroad, or from public or private research centers.

L'archive ouverte pluridisciplinaire **HAL**, est destinée au dépôt et à la diffusion de documents scientifiques de niveau recherche, publiés ou non, émanant des établissements d'enseignement et de recherche français ou étrangers, des laboratoires publics ou privés.



CERN-PH-EP-2014-033

LHCb-PAPER-2014-002

March,13 2014

Study of beauty hadron decays into pairs of charm hadrons

The LHCb collaboration[†]

Abstract

First observations of the decays $\Lambda_b^0 \rightarrow \Lambda_c^+ D_{(s)}^-$ are reported using data corresponding to an integrated luminosity of 3 fb^{-1} collected at 7 and 8 TeV center-of-mass energy in proton-proton collisions with the LHCb detector. In addition, the most precise measurement of the branching fraction $\mathcal{B}(B_s^0 \rightarrow D^+ D_s^-)$ is made and a search is performed for the decays $B_{(s)}^0 \rightarrow \Lambda_c^+ \Lambda_c^-$. The results obtained are

$$\begin{aligned} \mathcal{B}(\Lambda_b^0 \rightarrow \Lambda_c^+ D^-) / \mathcal{B}(\Lambda_b^0 \rightarrow \Lambda_c^+ D_s^-) &= 0.042 \pm 0.003 \text{ (stat)} \pm 0.003 \text{ (syst)}, \\ \left[\frac{\mathcal{B}(\Lambda_b^0 \rightarrow \Lambda_c^+ D_s^-)}{\mathcal{B}(\bar{B}^0 \rightarrow D^+ D_s^-)} \right] / \left[\frac{\mathcal{B}(\Lambda_b^0 \rightarrow \Lambda_c^+ \pi^-)}{\mathcal{B}(\bar{B}^0 \rightarrow D^+ \pi^-)} \right] &= 0.96 \pm 0.02 \text{ (stat)} \pm 0.06 \text{ (syst)}, \\ \mathcal{B}(B_s^0 \rightarrow D^+ D_s^-) / \mathcal{B}(\bar{B}^0 \rightarrow D^+ D_s^-) &= 0.038 \pm 0.004 \text{ (stat)} \pm 0.003 \text{ (syst)}, \\ \mathcal{B}(\bar{B}^0 \rightarrow \Lambda_c^+ \Lambda_c^-) / \mathcal{B}(\bar{B}^0 \rightarrow D^+ D_s^-) &< 0.0022 \text{ [95\% C.L.]}, \\ \mathcal{B}(B_s^0 \rightarrow \Lambda_c^+ \Lambda_c^-) / \mathcal{B}(B_s^0 \rightarrow D^+ D_s^-) &< 0.30 \text{ [95\% C.L.]}. \end{aligned}$$

Measurement of the mass of the Λ_b^0 baryon relative to the \bar{B}^0 meson gives $M(\Lambda_b^0) - M(\bar{B}^0) = 339.72 \pm 0.24 \text{ (stat)} \pm 0.18 \text{ (syst)} \text{ MeV}/c^2$. This result provides the most precise measurement of the mass of the Λ_b^0 baryon to date.

Submitted to Physical Review Letters.

© CERN on behalf of the LHCb collaboration, license CC-BY-3.0.

[†]Authors are listed on the following pages.

LHCb collaboration

R. Aaij⁴¹, A. Abba^{21,u}, B. Adeva³⁷, M. Adinolfi⁴⁶, A. Affolder⁵², Z. Ajaltouni⁵, J. Albrecht⁹, F. Alessio³⁸, M. Alexander⁵¹, S. Ali⁴¹, G. Alkhazov³⁰, P. Alvarez Cartelle³⁷, A.A. Alves Jr^{25,38}, S. Amato², S. Amerio²², Y. Amhis⁷, L. An³, L. Anderlini^{17,g}, J. Anderson⁴⁰, R. Andreassen⁵⁷, M. Andreotti^{16,f}, J.E. Andrews⁵⁸, R.B. Appleby⁵⁴, O. Aquines Gutierrez¹⁰, F. Archilli³⁸, A. Artamonov³⁵, M. Artuso⁵⁹, E. Aslanides⁶, G. Auriemma^{25,n}, M. Baalouch⁵, S. Bachmann¹¹, J.J. Back⁴⁸, A. Badalov³⁶, V. Balagura³¹, W. Baldini¹⁶, R.J. Barlow⁵⁴, C. Barschel³⁸, S. Barsuk⁷, W. Barter⁴⁷, V. Batozskaya²⁸, Th. Bauer⁴¹, A. Bay³⁹, J. Beddow⁵¹, F. Bedeschi²³, I. Bediaga¹, S. Belogurov³¹, K. Belous³⁵, I. Belyaev³¹, E. Ben-Haim⁸, G. Bencivenni¹⁸, S. Benson⁵⁰, J. Benton⁴⁶, A. Berezhnoy³², R. Bernet⁴⁰, M.-O. Bettler⁴⁷, M. van Beuzekom⁴¹, A. Bien¹¹, S. Bifani⁴⁵, T. Bird⁵⁴, A. Bizzeti^{17,i}, P.M. Bjørnstad⁵⁴, T. Blake⁴⁸, F. Blanc³⁹, J. Blouw¹⁰, S. Blusk⁵⁹, V. Bocci²⁵, A. Bondar³⁴, N. Bondar^{30,38}, W. Bonivento^{15,38}, S. Borghi⁵⁴, A. Borgia⁵⁹, M. Borsato⁷, T.J.V. Bowcock⁵², E. Bowen⁴⁰, C. Bozzi¹⁶, T. Brambach⁹, J. van den Brand⁴², J. Bressieux³⁹, D. Brett⁵⁴, M. Britsch¹⁰, T. Britton⁵⁹, N.H. Brook⁴⁶, H. Brown⁵², A. Bursche⁴⁰, G. Busetto^{22,q}, J. Buytaert³⁸, S. Cadeddu¹⁵, R. Calabrese^{16,f}, O. Callot⁷, M. Calvi^{20,k}, M. Calvo Gomez^{36,o}, A. Camboni³⁶, P. Campana^{18,38}, D. Campora Perez³⁸, F. Caponio^{21,u}, A. Carbone^{14,d}, G. Carboni^{24,l}, R. Cardinale^{19,38,j}, A. Cardini¹⁵, H. Carranza-Mejia⁵⁰, L. Carson⁵⁰, K. Carvalho Akiba², G. Casse⁵², L. Cassina²⁰, L. Castillo Garcia³⁸, M. Cattaneo³⁸, Ch. Cauet⁹, R. Cenci⁵⁸, M. Charles⁸, Ph. Charpentier³⁸, S.-F. Cheung⁵⁵, N. Chiapolini⁴⁰, M. Chrzaszcz^{40,26}, K. Ciba³⁸, X. Cid Vidal³⁸, G. Ciezarek⁵³, P.E.L. Clarke⁵⁰, M. Clemencic³⁸, H.V. Cliff⁴⁷, J. Closier³⁸, C. Coca²⁹, V. Coco³⁸, J. Cogan⁶, E. Cogneras⁵, P. Collins³⁸, A. Comerma-Montells³⁶, A. Contu^{15,38}, A. Cook⁴⁶, M. Coombes⁴⁶, S. Coquereau⁸, G. Corti³⁸, M. Corvo^{16,f}, I. Counts⁵⁶, B. Couturier³⁸, G.A. Cowan⁵⁰, D.C. Craik⁴⁸, M. Cruz Torres⁶⁰, A.R. Cukierman⁵⁶, S. Cunliffe⁵³, R. Currie⁵⁰, C. D'Ambrosio³⁸, J. Dalseno⁴⁶, P. David⁸, P.N.Y. David⁴¹, A. Davis⁵⁷, K. De Bruyn⁴¹, S. De Capua⁵⁴, M. De Cian¹¹, J.M. De Miranda¹, L. De Paula², W. De Silva⁵⁷, P. De Simone¹⁸, D. Decamp⁴, M. Deckenhoff⁹, L. Del Buono⁸, N. Déléage⁴, D. Derkach⁵⁵, O. Deschamps⁵, F. Dettori⁴², A. Di Canto³⁸, H. Dijkstra³⁸, S. Donleavy⁵², F. Dordei¹¹, M. Dorigo³⁹, C. Dorothy⁵⁶, A. Dosil Suárez³⁷, D. Dossett⁴⁸, A. Dovbnya⁴³, F. Dupertuis³⁹, P. Durante³⁸, R. Dzhelyadin³⁵, A. Dziurda²⁶, A. Dzyuba³⁰, S. Easo⁴⁹, U. Egede⁵³, V. Egorychev³¹, S. Eidelman³⁴, S. Eisenhardt⁵⁰, U. Eitschberger⁹, R. Ekelhof⁹, L. Eklund^{51,38}, I. El Rifai⁵, Ch. Elsasser⁴⁰, S. Esen¹¹, T. Evans⁵⁵, A. Falabella^{16,f}, C. Färber¹¹, C. Farinelli⁴¹, S. Farry⁵², D. Ferguson⁵⁰, V. Fernandez Albor³⁷, F. Ferreira Rodrigues¹, M. Ferro-Luzzi³⁸, S. Filippov³³, M. Fiore^{16,f}, M. Fiorini^{16,f}, M. Firlej²⁷, C. Fitzpatrick³⁸, T. Fiutowski²⁷, M. Fontana¹⁰, F. Fontanelli^{19,j}, R. Forty³⁸, O. Francisco², M. Frank³⁸, C. Frei³⁸, M. Frosini^{17,38,g}, J. Fu²¹, E. Furfaro^{24,l}, A. Gallas Torreira³⁷, D. Galli^{14,d}, S. Gambetta^{19,j}, M. Gandelman², P. Gandini⁵⁹, Y. Gao³, J. Garofoli⁵⁹, J. Garra Tico⁴⁷, L. Garrido³⁶, C. Gaspar³⁸, R. Gauld⁵⁵, L. Gavardi⁹, E. Gersabeck¹¹, M. Gersabeck⁵⁴, T. Gershon⁴⁸, Ph. Ghez⁴, A. Gianelle²², S. Giani³⁹, V. Gibson⁴⁷, L. Giubega²⁹, V.V. Gligorov³⁸, C. Göbel⁶⁰, D. Golubkov³¹, A. Golutvin^{53,31,38}, A. Gomes^{1,a}, H. Gordon³⁸, C. Gotti²⁰, M. Grabalosa Gándara⁵, R. Graciani Diaz³⁶, L.A. Granado Cardoso³⁸, E. Graugés³⁶, G. Graziani¹⁷, A. Grecu²⁹, E. Greening⁵⁵, S. Gregson⁴⁷, P. Griffith⁴⁵, L. Grillo¹¹, O. Grünberg⁶², B. Gui⁵⁹, E. Gushchin³³, Yu. Guz^{35,38}, T. Gys³⁸, C. Hadjivasiliou⁵⁹, G. Haefeli³⁹, C. Haen³⁸, S.C. Haines⁴⁷, S. Hall⁵³, B. Hamilton⁵⁸, T. Hampson⁴⁶, X. Han¹¹, S. Hansmann-Menzemer¹¹, N. Harnew⁵⁵, S.T. Harnew⁴⁶, J. Harrison⁵⁴, T. Hartmann⁶², J. He³⁸, T. Head³⁸, V. Heijne⁴¹, K. Hennessy⁵², P. Henrard⁵, L. Henry⁸,

J.A. Hernando Morata³⁷, E. van Herwijnen³⁸, M. Heß⁶², A. Hicheur¹, D. Hill⁵⁵, M. Hoballah⁵, C. Hombach⁵⁴, W. Hulsbergen⁴¹, P. Hunt⁵⁵, N. Hussain⁵⁵, D. Hutchcroft⁵², D. Hynds⁵¹, M. Idzik²⁷, P. Ilten⁵⁶, R. Jacobsson³⁸, A. Jaeger¹¹, J. Jalocha⁵⁵, E. Jans⁴¹, P. Jaton³⁹, A. Jawahery⁵⁸, M. Jezabek²⁶, F. Jing³, M. John⁵⁵, D. Johnson⁵⁵, C.R. Jones⁴⁷, C. Joram³⁸, B. Jost³⁸, N. Jurik⁵⁹, M. Kaballo⁹, S. Kandybei⁴³, W. Kango⁶, M. Karacson³⁸, T.M. Karbach³⁸, M. Kelsey⁵⁹, I.R. Kenyon⁴⁵, T. Ketel⁴², B. Khanji²⁰, C. Khurewathanakul³⁹, S. Klaver⁵⁴, O. Kochebina⁷, M. Kolpin¹¹, I. Komarov³⁹, R.F. Koopman⁴², P. Koppenburg^{41,38}, M. Korolev³², A. Kozlinskiy⁴¹, L. Kravchuk³³, K. Kreplin¹¹, M. Kreps⁴⁸, G. Krocker¹¹, P. Krovovny³⁴, F. Kruse⁹, M. Kucharczyk^{20,26,38,k}, V. Kudryavtsev³⁴, K. Kurek²⁸, T. Kvaratskheliya³¹, V.N. La Thi³⁹, D. Lacarrere³⁸, G. Lafferty⁵⁴, A. Lai¹⁵, D. Lambert⁵⁰, R.W. Lambert⁴², E. Lanciotti³⁸, G. Lanfranchi¹⁸, C. Langenbruch³⁸, B. Langhans³⁸, T. Latham⁴⁸, C. Lazzeroni⁴⁵, R. Le Gac⁶, J. van Leerdam⁴¹, J.-P. Lees⁴, R. Lefèvre⁵, A. Leflat³², J. Lefrançois⁷, S. Leo²³, O. Leroy⁶, T. Lesiak²⁶, B. Leverington¹¹, Y. Li³, M. Liles⁵², R. Lindner³⁸, C. Linn³⁸, F. Lionetto⁴⁰, B. Liu¹⁵, G. Liu³⁸, S. Lohn³⁸, I. Longstaff⁵¹, I. Longstaff⁵¹, J.H. Lopes², N. Lopez-March³⁹, P. Lowdon⁴⁰, H. Lu³, D. Lucchesi^{22,q}, H. Luo⁵⁰, A. Lupato²², E. Luppi^{16,f}, O. Lupton⁵⁵, F. Machefert⁷, I.V. Machikhiliyan³¹, F. Maciuc²⁹, O. Maev³⁰, S. Malde⁵⁵, G. Manca^{15,e}, G. Mancinelli⁶, M. Manzali^{16,f}, J. Maratas⁵, J.F. Marchand⁴, U. Marconi¹⁴, C. Marin Benito³⁶, P. Marino^{23,s}, R. Märki³⁹, J. Marks¹¹, G. Martellotti²⁵, A. Martens⁸, A. Martín Sánchez⁷, M. Martinelli⁴¹, D. Martinez Santos⁴², F. Martinez Vidal⁶⁴, D. Martins Tostes², A. Massafferri¹, R. Matev³⁸, Z. Mathe³⁸, C. Matteuzzi²⁰, A. Mazurov^{16,38,f}, M. McCann⁵³, J. McCarthy⁴⁵, A. McNab⁵⁴, R. McNulty¹², B. McSkelly⁵², B. Meadows^{57,55}, F. Meier⁹, M. Meissner¹¹, M. Merk⁴¹, D.A. Milanes⁸, M.-N. Minard⁴, J. Molina Rodriguez⁶⁰, S. Monteil⁵, D. Moran⁵⁴, M. Morandin²², P. Morawski²⁶, A. Mordà⁶, M.J. Morello^{23,s}, J. Moron²⁷, R. Mountain⁵⁹, F. Muheim⁵⁰, K. Müller⁴⁰, R. Muresan²⁹, B. Muster³⁹, P. Naik⁴⁶, T. Nakada³⁹, R. Nandakumar⁴⁹, I. Nasteva¹, M. Needham⁵⁰, N. Neri²¹, S. Neubert³⁸, N. Neufeld³⁸, M. Neuner¹¹, A.D. Nguyen³⁹, T.D. Nguyen³⁹, C. Nguyen-Mau^{39,p}, M. Nicol⁷, V. Niess⁵, R. Niet⁹, N. Nikitin³², T. Nikodem¹¹, A. Novoselov³⁵, A. Oblakowska-Mucha²⁷, V. Obraztsov³⁵, S. Oggero⁴¹, S. Ogilvy⁵¹, O. Okhrimenko⁴⁴, R. Oldeman^{15,e}, G. Onderwater⁶⁵, M. Orlandea²⁹, J.M. Otalora Goicochea², P. Owen⁵³, A. Oyanguren⁶⁴, B.K. Pal⁵⁹, A. Palano^{13,c}, F. Palombo^{21,t}, M. Palutan¹⁸, J. Panman³⁸, A. Papanestis^{49,38}, M. Pappagallo⁵¹, C. Parkes⁵⁴, C.J. Parkinson⁹, G. Passaleva¹⁷, G.D. Patel⁵², M. Patel⁵³, C. Patrignani^{19,j}, A. Pazos Alvarez³⁷, A. Pearce⁵⁴, A. Pellegrino⁴¹, M. Pepe Altarelli³⁸, S. Perazzini^{14,d}, E. Perez Trigo³⁷, P. Perret⁵, M. Perrin-Terrin⁶, L. Pescatore⁴⁵, E. Pesen⁶⁶, K. Petridis⁵³, A. Petrolini^{19,j}, E. Picatoste Olloqui³⁶, B. Pietrzyk⁴, T. Pilar⁴⁸, D. Pinci²⁵, A. Pistone¹⁹, S. Playfer⁵⁰, M. Plo Casasus³⁷, F. Polci⁸, A. Poluektov^{48,34}, E. Polycarpo², A. Popov³⁵, D. Popov¹⁰, B. Popovici²⁹, C. Potterat², A. Powell⁵⁵, J. Prisciandaro³⁹, A. Pritchard⁵², C. Prouve⁴⁶, V. Pugatch⁴⁴, A. Puig Navarro³⁹, G. Punzi^{23,r}, W. Qian⁴, B. Rachwal²⁶, J.H. Rademacker⁴⁶, B. Rakotomiaramanana³⁹, M. Rama¹⁸, M.S. Rangel², I. Raniuk⁴³, N. Rauschmayr³⁸, G. Raven⁴², S. Reichert⁵⁴, M.M. Reid⁴⁸, A.C. dos Reis¹, S. Ricciardi⁴⁹, A. Richards⁵³, K. Rinnert⁵², V. Rives Molina³⁶, D.A. Roa Romero⁵, P. Robbe⁷, A.B. Rodrigues¹, E. Rodrigues⁵⁴, P. Rodriguez Perez⁵⁴, S. Roiser³⁸, V. Romanovsky³⁵, A. Romero Vidal³⁷, M. Rotondo²², J. Rouvinet³⁹, T. Ruf³⁸, F. Ruffini²³, H. Ruiz³⁶, P. Ruiz Valls⁶⁴, G. Sabatino^{25,l}, J.J. Saborido Silva³⁷, N. Sagidova³⁰, P. Sail⁵¹, B. Saitta^{15,e}, V. Salustino Guimaraes², C. Sanchez Mayordomo⁶⁴, B. Sanmartin Sedes³⁷, R. Santacesaria²⁵, C. Santamarina Rios³⁷, E. Santovetti^{24,l}, M. Sapunov⁶, A. Sarti^{18,m}, C. Satriano^{25,n}, A. Satta²⁴, M. Savrie^{16,f}, D. Savrina^{31,32}, M. Schiller⁴², H. Schindler³⁸, M. Schlupp⁹, M. Schmelling¹⁰, B. Schmidt³⁸,

O. Schneider³⁹, A. Schopper³⁸, M.-H. Schune⁷, R. Schwemmer³⁸, B. Sciascia¹⁸, A. Sciubba²⁵, M. Seco³⁷, A. Semennikov³¹, K. Senderowska²⁷, I. Sepp⁵³, N. Serra⁴⁰, J. Serrano⁶, L. Sestini²², P. Seyfert¹¹, M. Shapkin³⁵, I. Shapoval^{16,43,f}, Y. Shcheglov³⁰, T. Shears⁵², L. Shekhtman³⁴, V. Shevchenko⁶³, A. Shires⁹, R. Silva Coutinho⁴⁸, G. Simi²², M. Sirendi⁴⁷, N. Skidmore⁴⁶, T. Skwarnicki⁵⁹, N.A. Smith⁵², E. Smith^{55,49}, E. Smith⁵³, J. Smith⁴⁷, M. Smith⁵⁴, H. Snoek⁴¹, M.D. Sokoloff⁵⁷, F.J.P. Soler⁵¹, F. Soomro³⁹, D. Souza⁴⁶, B. Souza De Paula², B. Spaan⁹, A. Sparkes⁵⁰, F. Spinella²³, P. Spradlin⁵¹, F. Stagni³⁸, S. Stahl¹¹, O. Steinkamp⁴⁰, O. Stenyakin³⁵, S. Stevenson⁵⁵, S. Stoica²⁹, S. Stone⁵⁹, B. Storaci⁴⁰, S. Stracka^{23,38}, M. Straticiuc²⁹, U. Straumann⁴⁰, R. Stroili²², V.K. Subbiah³⁸, L. Sun⁵⁷, W. Sutcliffe⁵³, K. Swientek²⁷, S. Swientek⁹, V. Syropoulos⁴², M. Szczekowski²⁸, P. Szczypka^{39,38}, D. Szilard², T. Szumlak²⁷, S. T'Jampens⁴, M. Teklishyn⁷, G. Tellarini^{16,f}, E. Teodorescu²⁹, F. Teubert³⁸, C. Thomas⁵⁵, E. Thomas³⁸, J. van Tilburg⁴¹, V. Tisserand⁴, M. Tobin³⁹, S. Tolk⁴², L. Tomassetti^{16,f}, D. Tonelli³⁸, S. Topp-Joergensen⁵⁵, N. Torr⁵⁵, E. Tournefier⁴, S. Tourneur³⁹, M.T. Tran³⁹, M. Tresch⁴⁰, A. Tsaregorodtsev⁶, P. Tsopelas⁴¹, N. Tuning⁴¹, M. Ubeda Garcia³⁸, A. Ukleja²⁸, A. Ustyuzhanin⁶³, U. Uwer¹¹, V. Vagnoni¹⁴, G. Valenti¹⁴, A. Vallier⁷, R. Vazquez Gomez¹⁸, P. Vazquez Regueiro³⁷, C. Vázquez Sierra³⁷, S. Vecchi¹⁶, J.J. Velthuis⁴⁶, M. Veltre^{17,h}, G. Veneziano³⁹, M. Vesterinen¹¹, B. Viaud⁷, D. Vieira², M. Vieites Diaz³⁷, X. Vilasis-Cardona^{36,o}, A. Vollhardt⁴⁰, D. Volyansky¹⁰, D. Voong⁴⁶, A. Vorobyev³⁰, V. Vorobyev³⁴, C. Voß⁶², H. Voss¹⁰, J.A. de Vries⁴¹, R. Waldi⁶², C. Wallace⁴⁸, R. Wallace¹², J. Walsh²³, S. Wandernoth¹¹, J. Wang⁵⁹, D.R. Ward⁴⁷, N.K. Watson⁴⁵, A.D. Webber⁵⁴, D. Websdale⁵³, M. Whitehead⁴⁸, J. Wicht³⁸, D. Wiedner¹¹, G. Wilkinson⁵⁵, M.P. Williams⁴⁵, M. Williams⁵⁶, F.F. Wilson⁴⁹, J. Wimberley⁵⁸, J. Wishahi⁹, W. Wislicki²⁸, M. Witek²⁶, G. Wormser⁷, S.A. Wotton⁴⁷, S. Wright⁴⁷, S. Wu³, K. Wyllie³⁸, Y. Xie⁶¹, Z. Xing⁵⁹, Z. Xu³⁹, Z. Yang³, X. Yuan³, O. Yushchenko³⁵, M. Zangoli¹⁴, M. Zavertyaev^{10,b}, F. Zhang³, L. Zhang⁵⁹, W.C. Zhang¹², Y. Zhang³, A. Zhelezov¹¹, A. Zhokhov³¹, L. Zhong³, A. Zvyagin³⁸.

¹Centro Brasileiro de Pesquisas Físicas (CBPF), Rio de Janeiro, Brazil

²Universidade Federal do Rio de Janeiro (UFRJ), Rio de Janeiro, Brazil

³Center for High Energy Physics, Tsinghua University, Beijing, China

⁴LAPP, Université de Savoie, CNRS/IN2P3, Annecy-Le-Vieux, France

⁵Clermont Université, Université Blaise Pascal, CNRS/IN2P3, LPC, Clermont-Ferrand, France

⁶CPPM, Aix-Marseille Université, CNRS/IN2P3, Marseille, France

⁷LAL, Université Paris-Sud, CNRS/IN2P3, Orsay, France

⁸LPNHE, Université Pierre et Marie Curie, Université Paris Diderot, CNRS/IN2P3, Paris, France

⁹Fakultät Physik, Technische Universität Dortmund, Dortmund, Germany

¹⁰Max-Planck-Institut für Kernphysik (MPIK), Heidelberg, Germany

¹¹Physikalisches Institut, Ruprecht-Karls-Universität Heidelberg, Heidelberg, Germany

¹²School of Physics, University College Dublin, Dublin, Ireland

¹³Sezione INFN di Bari, Bari, Italy

¹⁴Sezione INFN di Bologna, Bologna, Italy

¹⁵Sezione INFN di Cagliari, Cagliari, Italy

¹⁶Sezione INFN di Ferrara, Ferrara, Italy

¹⁷Sezione INFN di Firenze, Firenze, Italy

¹⁸Laboratori Nazionali dell'INFN di Frascati, Frascati, Italy

¹⁹Sezione INFN di Genova, Genova, Italy

²⁰Sezione INFN di Milano Bicocca, Milano, Italy

²¹Sezione INFN di Milano, Milano, Italy

²²Sezione INFN di Padova, Padova, Italy

²³Sezione INFN di Pisa, Pisa, Italy

- ²⁴Sezione INFN di Roma Tor Vergata, Roma, Italy
²⁵Sezione INFN di Roma La Sapienza, Roma, Italy
²⁶Henryk Niewodniczanski Institute of Nuclear Physics Polish Academy of Sciences, Kraków, Poland
²⁷AGH - University of Science and Technology, Faculty of Physics and Applied Computer Science, Kraków, Poland
²⁸National Center for Nuclear Research (NCBJ), Warsaw, Poland
²⁹Horia Hulubei National Institute of Physics and Nuclear Engineering, Bucharest-Magurele, Romania
³⁰Petersburg Nuclear Physics Institute (PNPI), Gatchina, Russia
³¹Institute of Theoretical and Experimental Physics (ITEP), Moscow, Russia
³²Institute of Nuclear Physics, Moscow State University (SINP MSU), Moscow, Russia
³³Institute for Nuclear Research of the Russian Academy of Sciences (INR RAN), Moscow, Russia
³⁴Budker Institute of Nuclear Physics (SB RAS) and Novosibirsk State University, Novosibirsk, Russia
³⁵Institute for High Energy Physics (IHEP), Protvino, Russia
³⁶Universitat de Barcelona, Barcelona, Spain
³⁷Universidad de Santiago de Compostela, Santiago de Compostela, Spain
³⁸European Organization for Nuclear Research (CERN), Geneva, Switzerland
³⁹Ecole Polytechnique Fédérale de Lausanne (EPFL), Lausanne, Switzerland
⁴⁰Physik-Institut, Universität Zürich, Zürich, Switzerland
⁴¹Nikhef National Institute for Subatomic Physics, Amsterdam, The Netherlands
⁴²Nikhef National Institute for Subatomic Physics and VU University Amsterdam, Amsterdam, The Netherlands
⁴³NSC Kharkiv Institute of Physics and Technology (NSC KIPT), Kharkiv, Ukraine
⁴⁴Institute for Nuclear Research of the National Academy of Sciences (KINR), Kyiv, Ukraine
⁴⁵University of Birmingham, Birmingham, United Kingdom
⁴⁶H.H. Wills Physics Laboratory, University of Bristol, Bristol, United Kingdom
⁴⁷Cavendish Laboratory, University of Cambridge, Cambridge, United Kingdom
⁴⁸Department of Physics, University of Warwick, Coventry, United Kingdom
⁴⁹STFC Rutherford Appleton Laboratory, Didcot, United Kingdom
⁵⁰School of Physics and Astronomy, University of Edinburgh, Edinburgh, United Kingdom
⁵¹School of Physics and Astronomy, University of Glasgow, Glasgow, United Kingdom
⁵²Oliver Lodge Laboratory, University of Liverpool, Liverpool, United Kingdom
⁵³Imperial College London, London, United Kingdom
⁵⁴School of Physics and Astronomy, University of Manchester, Manchester, United Kingdom
⁵⁵Department of Physics, University of Oxford, Oxford, United Kingdom
⁵⁶Massachusetts Institute of Technology, Cambridge, MA, United States
⁵⁷University of Cincinnati, Cincinnati, OH, United States
⁵⁸University of Maryland, College Park, MD, United States
⁵⁹Syracuse University, Syracuse, NY, United States
⁶⁰Pontifícia Universidade Católica do Rio de Janeiro (PUC-Rio), Rio de Janeiro, Brazil, associated to ²
⁶¹Institute of Particle Physics, Central China Normal University, Wuhan, Hubei, China, associated to ³
⁶²Institut für Physik, Universität Rostock, Rostock, Germany, associated to ¹¹
⁶³National Research Centre Kurchatov Institute, Moscow, Russia, associated to ³¹
⁶⁴Instituto de Fisica Corpuscular (IFIC), Universitat de Valencia-CSIC, Valencia, Spain, associated to ³⁶
⁶⁵KVI - University of Groningen, Groningen, The Netherlands, associated to ⁴¹
⁶⁶Celal Bayar University, Manisa, Turkey, associated to ³⁸

^aUniversidade Federal do Triângulo Mineiro (UFTM), Uberaba-MG, Brazil

^bP.N. Lebedev Physical Institute, Russian Academy of Science (LPI RAS), Moscow, Russia

^cUniversità di Bari, Bari, Italy

^dUniversità di Bologna, Bologna, Italy

^eUniversità di Cagliari, Cagliari, Italy

^fUniversità di Ferrara, Ferrara, Italy

- ^g Università di Firenze, Firenze, Italy
^h Università di Urbino, Urbino, Italy
ⁱ Università di Modena e Reggio Emilia, Modena, Italy
^j Università di Genova, Genova, Italy
^k Università di Milano Bicocca, Milano, Italy
^l Università di Roma Tor Vergata, Roma, Italy
^m Università di Roma La Sapienza, Roma, Italy
ⁿ Università della Basilicata, Potenza, Italy
^o LIFAELS, La Salle, Universitat Ramon Llull, Barcelona, Spain
^p Hanoi University of Science, Hanoi, Viet Nam
^q Università di Padova, Padova, Italy
^r Università di Pisa, Pisa, Italy
^s Scuola Normale Superiore, Pisa, Italy
^t Università degli Studi di Milano, Milano, Italy
^u Politecnico di Milano, Milano, Italy

Hadrons are systems of quarks bound by the strong interaction, described at the fundamental level by quantum chromodynamics (QCD). Low-energy phenomena, such as the binding of quarks and gluons within hadrons, lie in the nonperturbative regime of QCD and are difficult to calculate. Much progress has been made in recent years in the study of beauty mesons [1]; however, many aspects of beauty baryons are still largely unknown. Many decays of beauty mesons into pairs of charm hadrons have branching fractions at the percent level [2]. Decays of beauty baryons into pairs of charm hadrons are expected to be of comparable size, yet none have been observed to date. If such decays do have sizable branching fractions, they could be used to study beauty-baryon properties. For example, a comparison of beauty meson and baryon branching fractions can be used to test factorization in these decays.

Many models and techniques have been developed that attempt to reproduce the spectrum of the measured hadron masses, such as constituent quark models or lattice QCD calculations [3]. Precise measurements of ground-state beauty-baryon masses are required to permit precision tests of a variety of QCD models [4–10]. The Λ_b^0 baryon mass is particularly interesting in this context since several ground-state beauty-baryon masses are measured relative to that of the Λ_b^0 [11].

This Letter reports the first observation of the decays $\Lambda_b^0 \rightarrow \Lambda_c^+ D_s^-$ and $\Lambda_b^0 \rightarrow \Lambda_c^+ D^-$ made using data corresponding to an integrated luminosity of 1 and 2 fb^{-1} collected at 7 and 8 TeV center-of-mass energy in pp collisions, respectively, with the LHCb detector. The former is used to make the most precise measurement to date of the mass of the Λ_b^0 baryon. Improved measurements of the branching fraction $\mathcal{B}(B_s^0 \rightarrow D^+ D_s^-)$ and stringent upper limits on $\mathcal{B}(B_{(s)}^0 \rightarrow \Lambda_c^+ \Lambda_c^-)$ are also reported. Charge conjugated decay modes are implied throughout this Letter.

The LHCb detector [12] is a single-arm forward spectrometer covering the pseudo-rapidity range $2 < \eta < 5$, designed for the study of particles containing b or c quarks. The detector includes a high-precision tracking system consisting of a silicon-strip vertex detector surrounding the pp interaction region, a large-area silicon-strip detector located upstream of a dipole magnet with a bending power of about 4 Tm, and three stations of silicon-strip detectors and straw drift tubes [13] placed downstream. The combined tracking system provides a momentum measurement with relative uncertainty that varies from 0.4% at 5 GeV/c to 0.6% at 100 GeV/c, and impact parameter resolution of 20 μm for tracks with large transverse momentum (p_T). Different types of charged hadrons are distinguished by information from two ring-imaging Cherenkov detectors [14]. The hardware stage of the trigger uses information from calorimeter and muon systems [15]. The calorimeter system consists of scintillating-pad and preshower detectors, an electromagnetic calorimeter and a hadronic calorimeter. The muon system is composed of alternating layers of iron and multiwire proportional chambers [16]. The software stage of the trigger, which applies a full event reconstruction, uses a boosted decision tree (BDT) [17] to identify secondary vertices consistent with the decay of a beauty hadron [18].

Samples of simulated events are used to determine the signal selection efficiency, to model signal event distributions and to investigate possible background contributions. In the simulation, pp collisions are generated using PYTHIA [19] with a specific LHCb

configuration [20]. Decays of hadronic particles are described by EvtGen [21], in which final state radiation is generated using PHOTOS [22]. The interaction of the generated particles with the detector and its response are implemented using the GEANT4 toolkit [23] as described in Ref. [24].

In this analysis, signal beauty-hadron candidates are formed by combining charm-hadron candidate pairs reconstructed in the following decay modes: $D^+ \rightarrow K^-\pi^+\pi^+$, $D_s^+ \rightarrow K^-K^+\pi^+$ and $\Lambda_c^+ \rightarrow pK^-\pi^+$. The measured invariant mass of each charm-hadron candidate, the resolution on which is about $6-8\text{ MeV}/c^2$, is required to be within $25\text{ MeV}/c^2$ of the nominal value [2]. To improve the resolution of the beauty-hadron mass, the decay chain is fit imposing kinematic and vertex constraints [25]; this includes constraining the charm-hadron masses to their nominal values. To suppress contributions from non-charm decays, the reconstructed charm-hadron decay vertex is required to be downstream of and significantly displaced from the reconstructed beauty-hadron decay vertex.

A BDT is used to select each type of charm-hadron candidate. These BDTs use five variables for the charm hadron and 23 for each of its decay products. The variables include kinematic quantities, track and vertex qualities, and particle identification (PID) information. The signal and background samples used to train the BDTs are obtained from large samples of $\bar{B}^0 \rightarrow D^+\pi^-$, $\bar{B}_s^0 \rightarrow D_s^+\pi^-$ and $\Lambda_b^0 \rightarrow \Lambda_c^+\pi^-$ decays. These data samples are also used to validate selection efficiencies obtained from simulation. The signal distributions are background subtracted using weights [26] obtained from fits to the beauty-hadron invariant mass distributions. The background distributions are taken from the charm-hadron and high-mass beauty-hadron sidebands in the same data samples. To obtain the BDT efficiency in a given signal decay mode, the kinematical properties and correlations between the two charm hadrons are taken from simulation. The BDT response distributions are obtained from validation data samples of the decays used in the BDT training, weighted to match the kinematics of the signal.

Due to the kinematic similarity of the decays $D^+ \rightarrow K^-\pi^+\pi^+$, $D_s^+ \rightarrow K^-K^+\pi^+$ and $\Lambda_c^+ \rightarrow pK^-\pi^+$, cross-feed may occur among beauty-hadron decays into pairs of charm hadrons. For example, cross-feed between D^+ and D_s^+ mesons occurs when a $K^-h^+\pi^+$ candidate is reconstructed in the D^+ mass region under the $h^+ = \pi^+$ hypothesis and the D_s^+ mass region under the $h^+ = K^+$ hypothesis. In such situations, an arbitration is performed: if the ambiguous track (h^+) can be associated to an oppositely-charged track to form a $\phi(1020) \rightarrow K^+K^-$ candidate, the kaon hypothesis is taken resulting in a D_s^+ assignment to the charm-hadron candidate; otherwise, stringent PID requirements are applied to h^+ . The efficiency of these arbitrations is obtained using simulated signal decays to model the kinematical properties and $D^{*+} \rightarrow D^0\pi^+$ calibration data for the PID efficiencies.

Signal yields are determined by performing unbinned extended likelihood fits to the beauty-hadron invariant mass spectra observed in the data. The signal distributions are modeled using a so-called Apollonios function, which is the exponential of a hyperbola combined with a power-law low-mass tail [27]. The peak position and resolution parameters are allowed to vary while fitting the data, while the low-mass tail parameters are taken from simulation and fixed in the fits. The measurements reported in this paper are not

sensitive to the specific choice of the signal model.

Four categories of background contributions are considered: *partially reconstructed* decays of beauty hadrons where at least one final-state particle is not reconstructed; decays into a single charm hadron and three light hadrons; *reflections* where the cross-feed arbitration fails to remove a misidentified particle; and combinatorial background. The only partially reconstructed decays that contribute in the mass region studied are those where a single pion or photon is not reconstructed; thus, only final states comprised of $D_{(s)}^{*+}$ or Σ_c^+ and another charm hadron are considered (*e.g.*, $\Lambda_b^0 \rightarrow \Lambda_c^+ D_s^{*-}$). These background contributions are modeled using kernel probability density functions (PDFs) [28] obtained from simulation. Single-charm backgrounds are studied using data that are reconstructed outside of a given charm-hadron mass region and are found to be $\mathcal{O}(1\%)$ for decays containing a D_s^- (*e.g.*, $\bar{B}^0 \rightarrow D^+ K^- K^+ \pi^-$) and negligible otherwise. The only non-negligible reflection is found to be $\Lambda_b^0 \rightarrow \Lambda_c^+ D_s^-$ decays misidentified as $\Lambda_c^+ D^-$ candidates. The shape is obtained from simulation, while the normalization is fixed using simulation and the aforementioned PID calibration sample to determine the fraction of $\Lambda_b^0 \rightarrow \Lambda_c^+ D_s^-$ decays that are not removed by the cross-feed criteria. Reflections of $\bar{B}^0 \rightarrow D^+ D_s^-$ decays misidentified as final states containing Λ_c^+ particles do not have a peaking structure and, therefore, are absorbed into the combinatorial backgrounds, which are modeled using exponential distributions.

Figure 1 shows the invariant mass spectra for the $\Lambda_b^0 \rightarrow \Lambda_c^+ D_s^-$ and $\Lambda_b^0 \rightarrow \Lambda_c^+ D^-$ candidates. The signal yields obtained are 4633 ± 69 and 262 ± 19 for $\Lambda_b^0 \rightarrow \Lambda_c^+ D_s^-$ and $\Lambda_b^0 \rightarrow \Lambda_c^+ D^-$, respectively. This is the first observation of each of these decays. The ratio of branching fractions determined using the nominal D_s^- [2] and D^- [29] meson branching fractions and the ratio of efficiencies is

$$\frac{\mathcal{B}(\Lambda_b^0 \rightarrow \Lambda_c^+ D^-)}{\mathcal{B}(\Lambda_b^0 \rightarrow \Lambda_c^+ D_s^-)} = 0.042 \pm 0.003 \text{ (stat)} \pm 0.003 \text{ (syst)}.$$

The similarity of the final states and the shared parent particle result in many cancellations of uncertainties in the determination of the ratio of branching fractions. The remaining uncertainties include roughly equivalent contributions from determining the efficiency-corrected yields and from the ratio of charm-hadron branching fractions (see Table 1). The dominant contribution to the uncertainty of the fit PDF is due to the low-mass background contributions, which are varied in size and shape to determine the effect on the signal yield. The efficiencies of the cross-feed and BDT criteria are determined in a data-driven manner that produces small uncertainties. The observed ratio is approximately the ratio of the relevant quark-mixing factors and meson decay constants, $|V_{cd}/V_{cs}|^2 \times (f_D/f_{D_s})^2 \approx 0.034$, as expected assuming nonfactorizable effects are small.

The branching fraction of the decay $\Lambda_b^0 \rightarrow \Lambda_c^+ D_s^-$ is determined relative to that of the $\bar{B}^0 \rightarrow D^+ D_s^-$ decay. Using $D^+ D_s^-$ BDT criteria, optimized to maximize the expected \bar{B}^0 significance, $19\,395 \pm 145$ $\bar{B}^0 \rightarrow D^+ D_s^-$ decays are observed (see Fig. 2). The measurement of $\mathcal{B}(\Lambda_b^0 \rightarrow \Lambda_c^+ D_s^-)/\mathcal{B}(\bar{B}^0 \rightarrow D^+ D_s^-)$ is complicated by the fact that the ratio of the Λ_b^0 and \bar{B}^0 production cross sections, $\sigma(\Lambda_b^0)/\sigma(\bar{B}^0)$, depends on the p_T of the beauty hadrons [31]. Figure 3 shows the ratio of efficiency-corrected yields, $N(\Lambda_b^0 \rightarrow \Lambda_c^+ D_s^-)/N(\bar{B}^0 \rightarrow D^+ D_s^-)$,

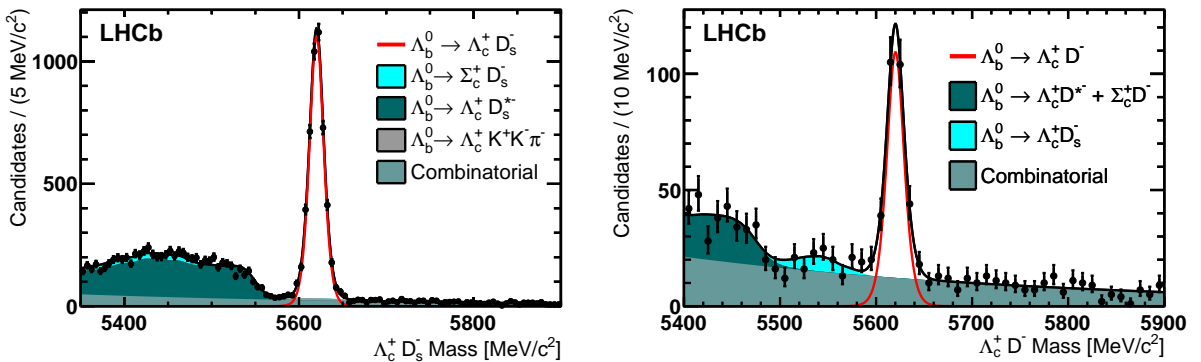


Figure 1: Invariant mass distributions for (left) $\Lambda_b^0 \rightarrow \Lambda_c^+ D_s^-$ and (right) $\Lambda_b^0 \rightarrow \Lambda_c^+ D^-$ candidates with the fits described in the text overlaid.

Table 1: Relative systematic uncertainties on branching fraction measurements (%). The production ratio $\sigma(B_s^0)/\sigma(\bar{B}^0)$ is taken from Ref. [30]. Numbers in brackets in the last column are for the B_s^0 decay mode.

Source	$\frac{\mathcal{B}(\Lambda_b^0 \rightarrow \Lambda_c^+ D^-)}{\mathcal{B}(\Lambda_b^0 \rightarrow \Lambda_c^+ D_s^-)}$	$\left[\frac{\mathcal{B}(\Lambda_b^0 \rightarrow \Lambda_c^+ D_s^-)}{\mathcal{B}(\bar{B}^0 \rightarrow D^+ D_s^-)} \right] / \left[\frac{\mathcal{B}(\Lambda_b^0 \rightarrow \Lambda_c^+ \pi^-)}{\mathcal{B}(\bar{B}^0 \rightarrow D^+ \pi^-)} \right]$	$\frac{\mathcal{B}(B_s^0 \rightarrow D^+ D_s^-)}{\mathcal{B}(\bar{B}^0 \rightarrow D^+ D_s^-)}$	$\frac{\mathcal{B}(B_{(s)}^0 \rightarrow \Lambda_c^+ \Lambda_c^-)}{\mathcal{B}(B_{(s)}^0 \rightarrow D^+ D_s^-)}$
Efficiency	3.5	5.2	1.0	3.9 (5.0)
Fit model	3.0	2.6	3.0	—
$\mathcal{B}(D_{(s)}^+, \Lambda_c^+)$	5.2	—	—	8.8
$\sigma(B_s^0)/\sigma(\bar{B}^0)$	—	—	5.8	—
Total	6.9	5.8	6.6	9.6 (10.1)

as a function of beauty-hadron p_T . The ratio of branching-fraction ratios is obtained using a fit with the shape of the p_T dependence measured in $\mathcal{B}(\Lambda_b^0 \rightarrow \Lambda_c^+ \pi^-)/\mathcal{B}(\bar{B}^0 \rightarrow D^+ \pi^-)$ [32] and found to be

$$\left[\frac{\mathcal{B}(\Lambda_b^0 \rightarrow \Lambda_c^+ D_s^-)}{\mathcal{B}(\bar{B}^0 \rightarrow D^+ D_s^-)} \right] / \left[\frac{\mathcal{B}(\Lambda_b^0 \rightarrow \Lambda_c^+ \pi^-)}{\mathcal{B}(\bar{B}^0 \rightarrow D^+ \pi^-)} \right] = 0.96 \pm 0.02 \text{ (stat)} \pm 0.06 \text{ (syst)}.$$

This result does not depend on the absolute ratio of production cross sections or on any charm-hadron branching fractions. The systematic uncertainties on this result are listed in Table 1. The uncertainty in the fit model is largely due to the sizable single-charm contributions to these modes and due to contributions from the fits described in Ref. [32]. The ratio $N(\Lambda_b^0 \rightarrow \Lambda_c^+ D_s^-)/N(\bar{B}^0 \rightarrow D^+ D_s^-)$ is observed to be consistent in data collected at $\sqrt{s} = 7$ and 8 TeV; thus, it is assumed that the production fractions of the Λ_b^0 and \bar{B}^0 are the same for all data analyzed and no systematic uncertainty is assigned. The ratio of branching ratios is consistent with unity as expected assuming small nonfactorizable effects.

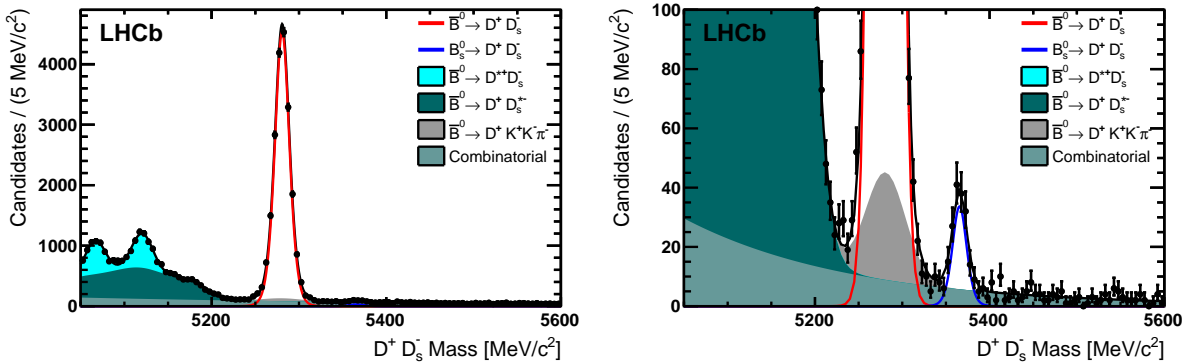


Figure 2: Invariant mass distributions for $D^+ D_s^-$ candidates selected using BDT criteria optimized for the (left) $B^0 \rightarrow D^+ D_s^-$ and (right) $B_s^0 \rightarrow D^+ D_s^-$ decay modes with the fits described in the text overlaid.

The kinematic similarity of the decay modes $\Lambda_b^0 \rightarrow \Lambda_c^+ D_s^-$ and $\bar{B}^0 \rightarrow D^+ D_s^-$ permits a precision measurement of the mass difference of the Λ_b^0 and \bar{B}^0 hadrons to be made. The relatively small value of $[M(\Lambda_b^0) - M(\Lambda_c^+) - M(D_s^-)] - [M(\bar{B}^0) - M(D^+) - M(D_s^-)]$ means that the uncertainty due to momentum scale, the dominant uncertainty in absolute mass measurements, mostly cancels; however, it is still important to determine accurately the momenta of the final state particles. The momentum scale calibration of the spectrometer, which accounts for imperfect knowledge of the magnetic field and alignment, is discussed in detail in Refs. [11, 33]. The uncertainty on the calibrated momentum scale is estimated to be 0.03% by comparing various particle masses measured at LHCb to their nominal values [33].

The kinematic and vertex constraints used in the fits described previously reduce the statistical uncertainty on $M(\Lambda_b^0) - M(\bar{B}^0)$ by improving the resolution. These constraints also increase the systematic uncertainty by introducing a dependence on the precision of the nominal charm-hadron masses. For this reason, these constraints are not imposed in the mass measurement. The mass difference obtained is

$$M(\Lambda_b^0) - M(\bar{B}^0) = 339.72 \pm 0.24 \text{ (stat)} \pm 0.18 \text{ (syst)} \text{ MeV}/c^2.$$

The dominant systematic uncertainty (see Table 2) arises due to a correlation between the reconstructed beauty-hadron mass and charm-hadron flight distance. The large difference in the Λ_c^+ and D^+ hadron lifetimes [2] causes only a partial cancelation of the biases induced by the charm-lifetime selection criteria. This effect is studied in simulation and a 0.16 MeV/c^2 uncertainty is assigned. The 0.03% uncertainty in the momentum scale results in an uncertainty on the mass difference of 0.08 MeV/c^2 . Many variations in the fit model are considered and none produce a significant shift in the mass difference. The systematic uncertainty in the mass difference due to the uncertainty in the amount of detector material in which charged particles lose energy is negligible [33]. Furthermore, the uncertainty on $M(\Lambda_b^0) - M(\bar{B}^0)$ due to differences in beauty-hadron production kinematics, as seen in Fig. 3, is also found to be negligible.

Table 2: Systematic uncertainties for $M(\Lambda_b^0) - M(\bar{B}^0)$.

Description	Value (MeV/ c^2)
$\Lambda_c^+ - D^+$ lifetime difference	0.16
Momentum scale	0.08
Fit model	0.02
Total	0.18

Using the nominal value for $M(\bar{B}^0)$ [2] gives $M(\Lambda_b^0) = 5619.30 \pm 0.34 \text{ MeV}/c^2$, where the uncertainty includes both statistical and systematic contributions. This is the most precise result to date. The total uncertainty is dominated by statistics and charm-hadron lifetime effects; thus, this result can be treated as being uncorrelated with the previous LHCb result obtained using the $\Lambda_b^0 \rightarrow J/\psi \Lambda^0$ decay [34]. A weighted average of the LHCb results gives $M(\Lambda_b^0) = 5619.36 \pm 0.26 \text{ MeV}/c^2$. This value may then be used to improve the precision of the Ξ_b^- and Ω_b^- baryon masses using their mass differences with respect to the Λ_b^0 baryon as reported in Ref. [34].

Using BDT criteria optimized for maximizing the expected significance of $B_s^0 \rightarrow D^+ D_s^-$, $14\,608 \pm 121$ \bar{B}^0 and 143 ± 14 B_s^0 decays are observed (see Fig. 2), from which the ratio extracted is

$$\frac{\mathcal{B}(B_s^0 \rightarrow D^+ D_s^-)}{\mathcal{B}(\bar{B}^0 \rightarrow D^+ D_s^-)} = 0.038 \pm 0.004 \text{ (stat)} \pm 0.003 \text{ (syst)}.$$

This yields the most precise measurement to date of $\mathcal{B}(B_s^0 \rightarrow D^+ D_s^-)$ and supersedes Ref. [35]. The systematic uncertainty is dominated by the contribution from beauty-hadron production fractions since the two decay modes share the same final state. The additional small efficiency uncertainty is due to the uncertainty on the B_s^0 lifetime. The fit model uncertainty is largely due to the size of the combinatorial background near the B_s^0 peak. The ratio of branching fractions is approximately the ratio of quark-mixing factors as expected assuming nonfactorizable effects are small.

A search is also performed for the decay modes $B_{(s)}^0 \rightarrow \Lambda_c^+ \Lambda_c^-$. Regions centered around the nominal beauty-meson masses with boundaries defined such that each region contains 95% of the corresponding signal are determined using simulation. The expected background contribution in each of these regions is obtained from the charm-hadron mass sidebands. Applying this technique to the $\bar{B}^0 \rightarrow D^+ D_s^-$ and $\Lambda_b^0 \rightarrow \Lambda_c^+ D_{(s)}^-$ decays produces background estimates consistent with those obtained by fitting the invariant mass spectra for those modes. No significant excess is observed in either $\Lambda_c^+ \Lambda_c^-$ signal region. The limits obtained using the method of Ref. [36] and the known D_s^- [2], D^- [29] and Λ_c^+ [37] hadron

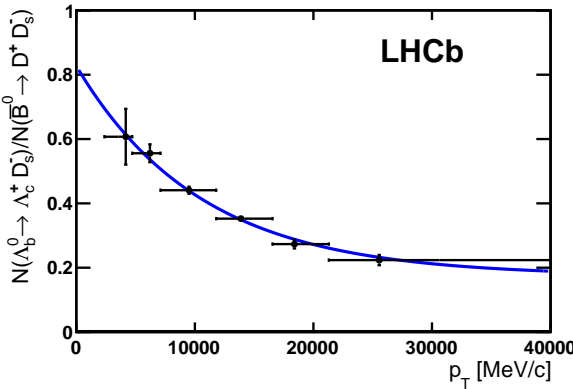


Figure 3: Efficiency-corrected yield ratio of $\Lambda_b^0 \rightarrow \Lambda_c^+ D_s^-$ to $\bar{B}^0 \rightarrow D^+ D_s^-$ vs p_T . The points are located at the mean p_T value of the Λ_b^0 in each bin. The curve shows the data fit with the shape of the p_T dependence measured in Ref. [32].

branching fractions are

$$\begin{aligned}\frac{\mathcal{B}(\bar{B}^0 \rightarrow \Lambda_c^+ \Lambda_c^-)}{\mathcal{B}(\bar{B}^0 \rightarrow D^+ D_s^-)} &< 0.0022 \text{ [95\% C.L.]}, \\ \frac{\mathcal{B}(B_s^0 \rightarrow \Lambda_c^+ \Lambda_c^-)}{\mathcal{B}(B_s^0 \rightarrow D^+ D_s^-)} &< 0.30 \text{ [95\% C.L.]}.\end{aligned}$$

For these results the lifetime of the light-mass B_s^0 eigenstate is assumed as this produces the most conservative limits [1]. This is the best limit to date for the \bar{B}^0 decay mode and the first limit for the B_s^0 decay mode.

In summary, first observations and relative branching fraction measurements have been made for the decays $\Lambda_b^0 \rightarrow \Lambda_c^+ D_{(s)}^-$. The most precise measurement of the Λ_b^0 baryon mass has been made via its mass difference relative to the \bar{B}^0 meson. The most precise measurement of $\mathcal{B}(B_s^0 \rightarrow D^+ D_s^-)$ has been presented and the most stringent upper limits have been placed on $\mathcal{B}(B_{(s)}^0 \rightarrow \Lambda_c^+ \Lambda_c^-)$. Using the PDG value $\mathcal{B}(\bar{B}^0 \rightarrow D^+ D_s^-) = (7.2 \pm 0.8) \times 10^{-3}$ [2] and the LHCb result for $\mathcal{B}(\Lambda_b^0 \rightarrow \Lambda_c^+ \pi^-)/\mathcal{B}(\bar{B}^0 \rightarrow D^+ \pi^-)$ [32], the absolute branching fractions obtained are

$$\begin{aligned}\mathcal{B}(\Lambda_b^0 \rightarrow \Lambda_c^+ D_s^-) &= (1.1 \pm 0.1) \times 10^{-2}, \\ \mathcal{B}(\Lambda_b^0 \rightarrow \Lambda_c^+ D^-) &= (4.7 \pm 0.6) \times 10^{-4}, \\ \mathcal{B}(B_s^0 \rightarrow D^+ D_s^-) &= (2.7 \pm 0.5) \times 10^{-4}, \\ \mathcal{B}(\bar{B}^0 \rightarrow \Lambda_c^+ \Lambda_c^-) &< 1.6 \times 10^{-5} \text{ [95\% C.L.]}, \\ \mathcal{B}(B_s^0 \rightarrow \Lambda_c^+ \Lambda_c^-) &< 8.0 \times 10^{-5} \text{ [95\% C.L.]}.\end{aligned}$$

These results are all consistent with expectations that assume small nonfactorizable effects.

Acknowledgements

We express our gratitude to our colleagues in the CERN accelerator departments for the excellent performance of the LHC. We thank the technical and administrative staff at the LHCb institutes. We acknowledge support from CERN and from the national agencies: CAPES, CNPq, FAPERJ and FINEP (Brazil); NSFC (China); CNRS/IN2P3 and Region Auvergne (France); BMBF, DFG, HGF and MPG (Germany); SFI (Ireland); INFN (Italy); FOM and NWO (The Netherlands); SCSR (Poland); MEN/IFA (Romania); MinES, Rosatom, RFBR and NRC “Kurchatov Institute” (Russia); MinECo, XuntaGal and GENCAT (Spain); SNSF and SER (Switzerland); NAS Ukraine (Ukraine); STFC (United Kingdom); NSF (USA). We also acknowledge the support received from EPLANET and the ERC under FP7. The Tier1 computing centres are supported by IN2P3 (France), KIT and BMBF (Germany), INFN (Italy), NWO and SURF (The Netherlands), PIC (Spain), GridPP (United Kingdom). We are indebted to the communities behind the multiple open source software packages we depend on. We are also thankful for the computing resources and the access to software R&D tools provided by Yandex LLC (Russia).

References

- [1] Heavy Flavor Averaging Group, Y. Amhis *et al.*, *Averages of b-hadron, c-hadron, and τ -lepton properties as of early 2012*, [arXiv:1207.1158](https://arxiv.org/abs/1207.1158), updated results and plots available at <http://www.slac.stanford.edu/xorg/hfag/>.
- [2] Particle Data Group, J. Beringer *et al.*, *Review of particle physics*, Phys. Rev. **D86** (2012) 010001, and 2013 partial update for the 2014 edition.
- [3] C. Amsler, T. Degrand, and B. Krusche, *Quark model*, published in Ref. [1].
- [4] M. Karliner, B. Keren-Zur, H. J. Lipkin, and J. L. Rosner, *The quark model and b baryons*, Annals Phys. **324** (2009) 2, [arXiv:0804.1575](https://arxiv.org/abs/0804.1575).
- [5] J. P. Day, W. Plessas, and K.-S. Choi, *Universal constituent-quark model for baryons*, [arXiv:1205.6918](https://arxiv.org/abs/1205.6918).
- [6] X. Liu *et al.*, *Bottom baryons*, Phys. Rev. **D77** (2008) 014031, [arXiv:0710.0123](https://arxiv.org/abs/0710.0123).
- [7] E. E. Jenkins, *Model-independent bottom baryon mass predictions in the $1/N_c$ expansion*, Phys. Rev. **D77** (2008) 034012, [arXiv:0712.0406](https://arxiv.org/abs/0712.0406).
- [8] R. Roncaglia, D. Lichtenberg, and E. Predazzi, *Predicting the masses of baryons containing one or two heavy quarks*, Phys. Rev. **D52** (1995) 1722, [arXiv:hep-ph/9502251](https://arxiv.org/abs/hep-ph/9502251).
- [9] N. Mathur, R. Lewis, and R. Woloshyn, *Charmed and bottom baryons from lattice NRQCD*, Phys. Rev. **D66** (2002) 014502, [arXiv:hep-ph/0203253](https://arxiv.org/abs/hep-ph/0203253).

- [10] D. Ebert, R. Faustov, and V. Galkin, *Masses of heavy baryons in the relativistic quark model*, Phys. Rev. **D72** (2005) 034026, [arXiv:hep-ph/0504112](#).
- [11] LHCb collaboration, R. Aaij *et al.*, *Measurement of b-hadron masses*, Phys. Lett. **B708** (2012) 241, [arXiv:1112.4896](#).
- [12] LHCb collaboration, A. A. Alves Jr. *et al.*, *The LHCb detector at the LHC*, JINST **3** (2008) S08005.
- [13] R. Arink *et al.*, *Performance of the LHCb Outer Tracker*, JINST **9** (2014) P01002, [arXiv:1311.3893](#).
- [14] M. Adinolfi *et al.*, *Performance of the LHCb RICH detector at the LHC*, Eur. Phys. J. **C73** (2013) 2431, [arXiv:1211.6759](#).
- [15] R. Aaij *et al.*, *The LHCb trigger and its performance in 2011*, JINST **8** (2013) P04022, [arXiv:1211.3055](#).
- [16] A. A. Alves Jr. *et al.*, *Performance of the LHCb muon system*, JINST **8** (2013) P02022, [arXiv:1211.1346](#).
- [17] L. Breiman, J. H. Friedman, R. A. Olshen, and C. J. Stone, *Classification and regression trees*, Wadsworth international group, Belmont, California, USA, 1984.
- [18] V. V. Gligorov and M. Williams, *Efficient, reliable and fast high-level triggering using a bonsai boosted decision tree*, JINST **8** (2013) P02013, [arXiv:1210.6861](#).
- [19] T. Sjöstrand, S. Mrenna, and P. Skands, *PYTHIA 6.4 physics and manual*, JHEP **05** (2006) 026, [arXiv:hep-ph/0603175](#); T. Sjöstrand, S. Mrenna, and P. Skands, *A brief introduction to PYTHIA 8.1*, Comput. Phys. Commun. **178** (2008) 852, [arXiv:0710.3820](#).
- [20] I. Belyaev *et al.*, *Handling of the generation of primary events in GAUSS, the LHCb simulation framework*, Nuclear Science Symposium Conference Record (NSS/MIC) IEEE (2010) 1155.
- [21] D. J. Lange, *The EvtGen particle decay simulation package*, Nucl. Instrum. Meth. **A462** (2001) 152.
- [22] P. Golonka and Z. Was, *PHOTOS Monte Carlo: a precision tool for QED corrections in Z and W decays*, Eur. Phys. J. **C45** (2006) 97, [arXiv:hep-ph/0506026](#).
- [23] Geant4 collaboration, J. Allison *et al.*, *Geant4 developments and applications*, IEEE Trans. Nucl. Sci. **53** (2006) 270; Geant4 collaboration, S. Agostinelli *et al.*, *Geant4: a simulation toolkit*, Nucl. Instrum. Meth. **A506** (2003) 250.
- [24] M. Clemencic *et al.*, *The LHCb simulation application, GAUSS: design, evolution and experience*, J. Phys. Conf. Ser. **331** (2011) 032023.

- [25] W. D. Hulsbergen, *Decay chain fitting with a Kalman filter*, Nucl. Instrum. Meth. **A552** (2005) 566, [arXiv:physics/0503191](#).
- [26] M. Pivk and F. R. Le Diberder, *sPlot: a statistical tool to unfold data distributions*, Nucl. Instrum. Meth. **A555** (2005) 356, [arXiv:physics/0402083](#).
- [27] D. M. Santos and F. Dupertuis, *Mass distributions marginalized over per-event errors*, Submitted to NIM (2013) [arXiv:1312.5000](#).
- [28] K. S. Cranmer, *Kernel estimation in high-energy physics*, Comput. Phys. Commun. **136** (2001) 198, [arXiv:hep-ex/0011057](#).
- [29] CLEO collaboration, G. Bonvicini *et al.*, *Updated measurements of absolute D^+ and D^0 hadronic branching fractions and $\sigma(e^+e^- \rightarrow D\bar{D})$ at $E_{\text{cm}} = 3774$ MeV*, [arXiv:1312.6775](#).
- [30] LHCb collaboration, *Updated average f_s/f_d b-hadron production fraction ratio for 7 TeV pp collisions*, LHCb-CONF-2013-011.
- [31] LHCb collaboration, R. Aaij *et al.*, *Measurement of b hadron production fractions in 7 TeV pp collisions*, Phys. Rev. **D85** (2012) 032008, [arXiv:1111.2357](#).
- [32] LHCb collaboration, R. Aaij *et al.*, *Measurement of the p_T and η dependences of Λ_b^0 production and the $\Lambda_b^0 \rightarrow \Lambda_c^+\pi^-$ branching fraction*, LHCb-PAPER-2014-004, in preparation.
- [33] LHCb collaboration, R. Aaij *et al.*, *Precision measurements of D meson mass differences*, JHEP **06** (2013) 65, [arXiv:1304.6865](#).
- [34] LHCb collaboration, R. Aaij *et al.*, *Measurements of the Λ_b^0 , Ξ_b^- and Ω_b^- baryon masses*, Phys. Rev. Lett. **110** (2013) 182001, [arXiv:1302.1072](#).
- [35] LHCb collaboration, R. Aaij *et al.*, *First observations of $\overline{B}_s^0 \rightarrow D^+D^-$, $D_s^+D^-$ and $D^0\overline{D}^0$ decays*, Phys. Rev. **D87** (2013) 092007, [arXiv:1302.5854](#).
- [36] W. A. Rolke, A. M. Lopez, and J. Conrad, *Limits and confidence intervals in the presence of nuisance parameters*, Nucl. Instrum. Meth. **A551** (2005) 493, [arXiv:physics/0403059](#).
- [37] Belle collaboration, A. Zupanc *et al.*, *Measurement of the branching fraction $\mathcal{B}(\Lambda_c^+ \rightarrow pK^-\pi^+)$* , [arXiv:1312.7826](#).